INSTITUTE OF PHYSICS PUBLISHING JOURNAL OF OPTICS A: PURE AND APPLIED OPTICS
J. Opt. A: Pure Appl. Opt. **7** (2005) 685–690 doi:10.1088/1464-4258/7/11/011

Orbital and spin angular momentum in conical diffraction

M V Berry[1], M R Jeffrey[1] and M Mansuripur[2]

[1] H H Wills Physics Laboratory, Tyndall Avenue, Bristol BS8 1TL, UK
[2] College of Optical Sciences, The University of Arizona, Tucson, AZ 85721, USA

Received 19 July 2005, accepted for publication 5 September 2005
Published 18 October 2005
Online at stacks.iop.org/JOptA/7/685

Abstract
The angular momentum $J_{\rm inc}$ of a light beam can be changed by passage through a slab of crystal. When the beam is incident along the optic axis of a biaxial crystal, which may also possess optical activity (chirality), the final angular momentum J can have both orbital ($J_{\rm orb}$) and spin ($J_{\rm sp}$) contributions, which we calculate paraxially exactly for arbitrary biaxiality and chirality and initially uniformly polarized beams with circular symmetry. For the familiar special case of a non-chiral crystal with fully developed conical-refraction rings, J is purely orbital and equal to $J_{\rm inc}/2$, reflecting an interesting singularity structure in the beam. Explicit formulas and numerical computations are presented for a Gaussian incident beam. The change in angular momentum results in a torque on the crystal, along the axis of the incident beam. An additional, much larger, torque, about an axis lying in the slab, arises from the offset of the cone of conical refraction relative to the incident beam.

Keywords: polarization, crystal optics, singularities

1. Introduction

In recent years, interest in the angular momentum of light has revived, partly because of the understanding [1] that light possesses orbital angular momentum, associated with the spatial distribution of the fields, in addition to the spin angular momentum associated with the polarization. For fields with simple symmetry (e.g. Laguerre–Gauss beams), the angular momentum is associated with optical singularities—another focus of current interest [2].

Here we study the angular momentum (orbital and spin) for a highly singular situation that was important in the development of optics [3–6] and remains interesting [7–9]. This is the wave field associated with conical refraction, in which a narrow light beam is incident along an optic axis of a slab of biaxial crystal, which may also possess chirality (optical activity). The beam spreads into a hollow cone inside the slab, and emerges as a hollow cylinder (figure 1). The detailed structure of the cylinder requires the solution of a diffraction problem (section 2), and depends on the distance from the slab, the ratio of the cylinder radius to the width of the incident beam, and the amount of chirality [8].

The main results (section 3) are explicit formulas for the orbital angular momentum $J_{\rm orb}$ and the spin angular momentum $J_{\rm sp}$ of the emergent beam, and the total angular momentum $J = J_{\rm orb} + J_{\rm sp}$. The emerging angular momenta differ from the incident ones by a factor that depends on the crystal parameters, indicating a torque tending to twist the slab in its own plane. For an incident beam with circular symmetry (in amplitude and therefore intensity), the incident angular momentum is entirely spin, i.e. $J_{\rm orb} = 0$, yet the emerging angular momentum generally contains both $J_{\rm orb}$ and $J_{\rm sp}$. In important limiting cases (section 4) the formulas simplify. Of these, the most interesting (section 4.1) is that originally predicted by Hamilton [3], where there is no chirality and the rings are fully developed. Then the incident spin angular momentum has been transformed entirely to orbital and reduced by a factor of two. The calculation is exact in the paraxial regime, which holds for all cases of conical refraction studied until now.

The calculation of section 3 is based on the following formula [1, 10] for the component along z (incident beam direction, with z measured from the entrance face of the crystal) of the angular momentum per photon, involving the transverse field $\mathbf{E}(\mathbf{R}, z) = \{E_x(\mathbf{R}, z), E_y(\mathbf{R}, z)\}$, with $\mathbf{R} = \{x, y\} = \{R\cos\phi, R\sin\phi\}$:

$$J = \frac{\hbar\,\mathrm{Im}\int\int \mathrm{d}\mathbf{R}(\mathbf{E}^*\cdot\partial_\phi\mathbf{E} + \mathbf{e}_z\cdot\mathbf{E}^*\times\mathbf{E})}{\int\int \mathrm{d}\mathbf{R}\,\mathbf{E}^*\cdot\mathbf{E}} \equiv J_{\rm orb} + J_{\rm sp}. \quad (1)$$

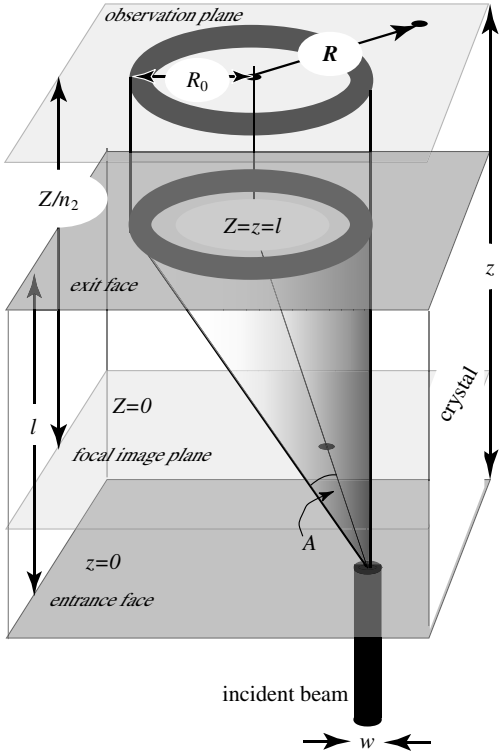

Figure 1. Geometry and coordinates as explained in the text, for an incident beam of width w, forming a cone with semi-angle A inside a biaxial crystal of thickness l and mean refractive index n_2, and emerging as a ring system whose dark ring has radius R_0.

The first term, involving the azimuthal derivative ∂_ϕ, is the integral over the emergent beam of the local expectation value of the orbital angular momentum operator $\mathbf{R} \times (-\mathrm{i}\hbar\nabla)$. The second term is the expectation of the spin angular momentum operator (for Cartesian field components) $\hbar\boldsymbol{\sigma}_2$, where $\boldsymbol{\sigma}_2$ is the second Pauli matrix.

2. Conical diffracted emergent field

Consider a transparent crystal with thickness l and three principal refractive indices

$$n_1 < n_2 < n_3 \tag{2}$$

with $n_2 - n_1 \ll 1$ and $n_3 - n_2 \ll 1$, reflecting paraxiality. We work with the crystal wavenumber k, defined in terms of the vacuum wavenumber k_0 by

$$k \equiv n_2 k_0. \tag{3}$$

The semi-angle of the geometrical cone inside the crystal is [6, 11]

$$A = \frac{1}{n_2}\sqrt{(n_2 - n_1)(n_3 - n_2)}. \tag{4}$$

In addition, the crystal may possess chirality, described by the parameter Γ, where $kl\Gamma$ is the angle through which the linear polarization of a plane wave, travelling along the optic axis, is rotated by the crystal.

The effect of such a crystal on light can be described compactly by the Hamiltonian operator (an obvious generalization, to incorporate chirality, of that derived in [9]) describing propagation inside ($z < l$) and outside ($z > l$) the crystal:

$$\mathsf{H}(\mathbf{P}) = [\tfrac{1}{2}P^2\mathbf{1} + \mathbf{S}\cdot\mathbf{Q}]\Theta(l - z) + \tfrac{1}{2}n_2 P^2\mathbf{1}\Theta(z - l). \tag{5}$$

Here the transverse momentum $\mathbf{P} = \{k_x, k_y\}/k$ is the dimensionless transverse wavevector of plane waves $\mathbf{k} = \{k_x, k_y, k_z\}$, and Θ denotes the unit step. The operator $\mathbf{S}$ and vector $\mathbf{Q}$ denote

$$\mathbf{S} = \{\boldsymbol{\sigma}_3, \boldsymbol{\sigma}_1, \boldsymbol{\sigma}_2\}, \qquad \mathbf{Q} = \{AP_x, AP_y, \Gamma\}. \tag{6}$$

The operator H acts on the incident field to give the field at any distance z, according to

$$\mathbf{E}(\mathbf{R}, z) = \exp\left\{-\mathrm{i}k\int_0^z \mathrm{d}z'\ \mathsf{H}(\mathbf{P}, z')\right\}\mathbf{E}(\mathbf{R}, 0). \tag{7}$$

For simplicity we assume that the incident field is uniformly polarized and has circular symmetry, with amplitude profile $E_0(R)$. Thus it can be written as a Bessel superposition of plane waves labelled by P, with strength $a(P)$:

$$\mathbf{E}(\mathbf{R}, 0) = E_0(R)\mathbf{e}_0 = \int_0^\infty \mathrm{d}P\,P a(P) J_0(kRP)\mathbf{e}_0, \tag{8}$$

where

$$a(P) = k^2\int_0^\infty \mathrm{d}R\,R E_0(R) J_0(kRP) \tag{9}$$

and the normalized initial polarization is

$$\mathbf{e}_0 = \begin{pmatrix} e_{x0} \\ e_{y0} \end{pmatrix}, \qquad \text{where } \mathbf{e}_0^*\cdot\mathbf{e}_0 = |e_{x0}|^2 + |e_{y0}|^2 = 1. \tag{10}$$

We are interested in the wave outside the crystal, for which it is convenient to define

$$R_0 \equiv Al, \qquad G \equiv \Gamma l, \qquad Z \equiv l + (z - l)n_2. \tag{11}$$

Here R_0 is the radius of the cylinder of refraction beyond the crystal (figure 1), G is the accumulated chirality, and Z measures distance, in units of n_2, from the focal image plane (this would be the virtual image plane of the entrance face if the crystal were isotropic with index n_2). Thus $Z = 0$ corresponds to $z = l(1 - 1/n_2)$ (image of entrance face), and $Z = l$ corresponds to $z = l$ (exit face).

From (7), it follows after a little calculation that the wave at $\{\mathbf{R}, Z\}$ outside the crystal is

$$\mathbf{E}(\mathbf{R}, Z) = [B_0(R, Z)\mathbf{1} + \mathbf{C}(R, Z)\cdot\mathbf{S}]\mathbf{e}_0, \tag{12}$$

where

$$\mathbf{C}(R, Z) = \{B_1(R, Z)\cos\phi, B_1(R, Z)\sin\phi, B_2(R, Z)\}, \tag{13}$$

and B_0 and B_1 and B_2 are the integrals:

$$\begin{aligned}
B_0(R, Z) &= \int_0^\infty \mathrm{d}P\,P[a(P)\exp\{-\tfrac{1}{2}\mathrm{i}kZP^2\} \\
&\quad\times \cos\left(k\sqrt{R_0^2P^2 + G^2}\right)J_0(kRP)], \\
B_1(R, Z) &= \int_0^\infty \mathrm{d}P\,P\frac{PR_0}{\sqrt{R_0^2P^2 + G^2}}\left[a(P)\exp\left\{-\frac{1}{2}\mathrm{i}kZP^2\right\}\right. \\
&\quad\left.\times \sin\left(k\sqrt{R_0^2P^2 + G^2}\right)J_1(kRP)\right], \\
B_2(R, Z) &= \mathrm{i}\int_0^\infty \mathrm{d}P\,P\frac{G}{\sqrt{R_0^2P^2 + G^2}}\left[a(P)\exp\left\{-\frac{1}{2}\mathrm{i}kZP^2\right\}\right. \\
&\quad\left.\times \sin\left(k\sqrt{R_0^2P^2 + G^2}\right)J_0(kRP)\right].
\end{aligned} \tag{14}$$

Although described differently, these are the same integrals as in the pioneering exact paraxial theory of Belsky *et al* [7, 8], equivalent to that based on (5).

3. Angular momentum

The angular momentum of the incident beam, easily calculated from (1) and (8), is

$$J_{\rm inc} = 2\hbar\,{\rm Im}\,e^*_{x0}e_{y0}. \tag{15}$$

For example, with circularly polarized incident light, where $\mathbf{e}_0 = \{1, \pm{\rm i}\}/\sqrt{2}$, $J_{\rm inc} = \pm\hbar$, and for linearly polarized light (e_y/e_x real) $J_{\rm inc} = 0$.

Calculation of the angular momenta in the emergent beam is a straightforward but lengthy exercise starting from (1) and the field (12). The integration over the angle ϕ eliminates many terms, and those that remain, involving the integrals (4), are greatly simplified by Bessel-transform identities. The results, independent of Z as they must be, are

$$J_{\rm orb} = \frac{J_{\rm inc}}{\int_0^\infty {\rm d}P\,P\,|a(P)|^2}\int_0^\infty {\rm d}P\,P\,|a(P)|^2\frac{R_0^2P^2}{R_0^2P^2+G^2} \times \sin^2\Big(k\sqrt{R_0^2P^2+G^2}\Big), \tag{16}$$

$$J_{\rm sp} = \frac{J_{\rm inc}}{\int_0^\infty {\rm d}P\,P\,|a(P)|^2} \times \int_0^\infty {\rm d}P\,P\,|a(P)|^2\Big[\cos^2\Big(k\sqrt{R_0^2P^2+G^2}\Big) + \frac{G^2-R_0^2P^2}{G^2+R_0^2P^2}\sin^2\Big(k\sqrt{R_0^2P^2+G^2}\Big)\Big], \tag{17}$$

$$J = \frac{J_{\rm inc}}{\int_0^\infty {\rm d}P\,P\,|a(P)|^2} \times \int_0^\infty {\rm d}P\,P\,|a(P)|^2\Big[\cos^2\Big(k\sqrt{R_0^2P^2+G^2}\Big) + \frac{G^2}{G^2+R_0^2P^2}\sin^2\Big(k\sqrt{R_0^2P^2+G^2}\Big)\Big]. \tag{18}$$

If the initial beam is Gaussian, that is

$$E_0(R) = \exp\Big(-\frac{R^2}{2w^2}\Big), \qquad a(P) = k^2w^2\exp\big(-\tfrac{1}{2}k^2P^2w^2\big), \tag{19}$$

these formulas can be written more simply using the scaled cylinder and chirality variables

$$\rho_0 \equiv \frac{R_0}{w}, \qquad \gamma \equiv kG. \tag{20}$$

After some manipulation, we obtain

$$\begin{aligned} J_{\rm orb} &= \tfrac{1}{2}J_{\rm inc}\big[1 - (\gamma/\rho_0)^2\exp\{(\gamma/\rho_0)^2\}E_1\{(\gamma/\rho_0)^2\} - F(\rho_0,\gamma)\big] \\ J_{\rm sp} &= J_{\rm inc}[(\gamma/\rho_0)^2\exp\{(\gamma/\rho_0)^2\}E_1\{(\gamma/\rho_0)^2\} + F(\rho_0,\gamma)] \\ J &= \tfrac{1}{2}J_{\rm inc}[1 + (\gamma/\rho_0)^2\exp\{(\gamma/\rho_0)^2\}E_1\{(\gamma/\rho_0)^2\} + F(\rho_0,\gamma)]. \end{aligned} \tag{21}$$

Here E_1 is the exponential integral

$$E_1(x) \equiv \int_x^\infty \frac{{\rm d}t}{t}\exp(-t) \tag{22}$$

[12], and

$$F(\rho_0,\gamma) = 2\exp((\gamma/\rho_0)^2) \times \int_{\gamma/\rho_0}^\infty {\rm d}t\Big[t - \frac{(\gamma/\rho_0)^2}{t}\Big]\exp(-t^2)\cos(2\rho_0 t). \tag{23}$$

(F can be expressed in terms of the error erf and an integral involving erf, but we have not found this representation useful.)

The formulas (21), and their more general versions (16)–(18), are our main results. Their content is illustrated in figure 2, showing $J_{\rm orb}$, $J_{\rm sp}$ and J as functions of the two crystal parameters. To understand the results, we now turn to special cases.

4. Special cases

4.1. Well developed rings, no chirality

This case, where $\rho_0 \gg 1$, $\gamma = 0$, is the most familiar conical refraction situation [3, 4], for which the general formula (21) simplifies:

$$J_{\rm orb} = \tfrac{1}{2}J_{\rm inc}, \qquad J_{\rm sp} = 0, \qquad J = \tfrac{1}{2}J_{\rm inc}, \tag{24}$$

indicating that the crystal has reduced the angular momentum to half its initial value (15), and transformed it to purely orbital, whatever the initial state.

This result, surprising at first sight, can be understood in physical terms. For well developed rings, the polarization at any point is linear, as was understood by the pioneers [3–5], and as follows from (12) to (14) with $\gamma = 0$ and $\rho_0 \gg 1$, when $B_2 = 0$ and $B_0 \sim B_1$ [9]. The polarization direction is independent of radial position R and depends only on azimuth ϕ, and rotates by π around the rings (figure 3). For pure linear polarization, $J_{\rm sp} = 0$, and $J_{\rm orb}$ can be calculated from (1) simply from the angular dependence of the field, which, as follows from (12) to (14), is proportional to

$$\mathbf{e}(\phi) = [e_x\cos(\tfrac{1}{2}\phi) + e_y\sin(\tfrac{1}{2}\phi)]\begin{pmatrix}\cos(\frac{1}{2}\phi)\\ \sin(\frac{1}{2}\phi)\end{pmatrix}. \tag{25}$$

For this case, $J_{\rm orb}$ is proportional to the geometric phase accumulated by the polarization around the rings (in general, $J_{\rm orb}$ is a radially weighted average of the phase). For circular incident polarization, the factor 1/2 reflects the fact that the π polarization rotation is accompanied by a π phase rotation. Then, from the perspective of singular optics, the polarization pattern of figure 3 is a manifestation of a C (i.e. circular) polarization singularity with index +1/2 [13–16]. To understand this, it is necessary to consider points well inside the rings, where the light intensity is very small and the approximation (25) does not hold. The polarization is elliptic, and must be circular somewhere, namely at the C point (if the incident beam is circularly polarized, the C point is at $R = 0$). The unexpected outcome is a polarization singularity with half-integer *orbital* angular momentum.

4.2. Chirality dominates

This is the opposite situation. When $\gamma \gg \rho_0$, (21) reduces to

$$J_{\rm orb} = 0, \qquad J_{\rm sp} = J = J_{\rm inc}, \tag{26}$$

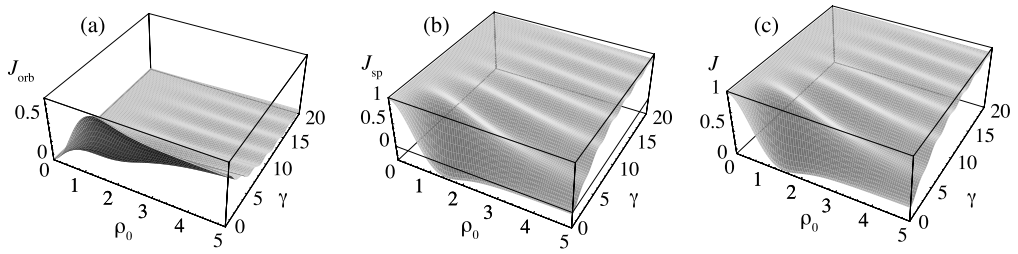

Figure 2. Angular momenta (a) J_{orb}; (b) J_{sp}; (c) $J = J_{orb} + J_{sp}$, as functions of the cylinder radius and chirality parameters ρ_0 and γ, computed by numerical integration of (21).

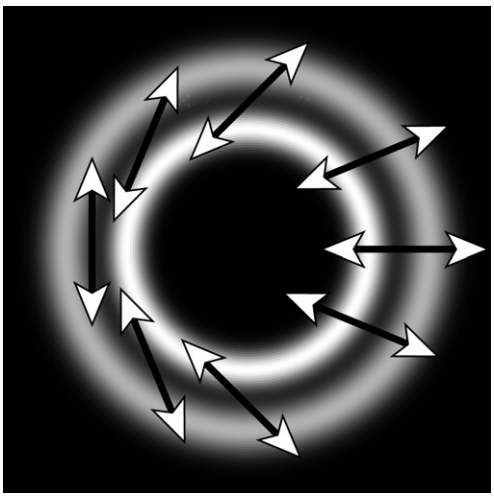

Figure 3. Linear polarization everywhere for well developed rings (section 4.1), dependent on azimuth but not radius.

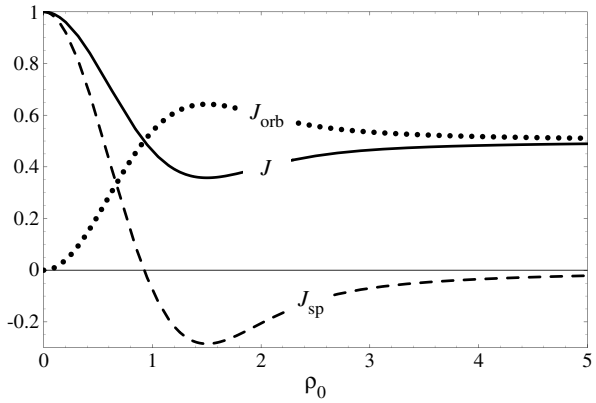

Figure 4. Angular momenta as a function of scaled cylinder radius ρ_0, for zero chirality, calculated from (27).

indicating that for strong chirality the crystal changes only the phases of the circular components of the incident beam and so has no effect on its angular momentum. (In (12)–(14), this corresponds to $B_1 = 0$, $B_0 \sim \cos(kG)$, $B_2 \sim i\sin(kG)$.)

4.3. Arbitrary biaxiality, no chirality

This is the case of partially developed conical refraction rings, where $\gamma = 0$ and ρ_0 can have any value [9]. Equation (21) takes the simpler form

$$\begin{aligned} J_{orb} &= \tfrac{1}{2} J_{inc}\rho_0 \exp(-\rho_0^2)\sqrt{\pi}\,\mathrm{erfi}(\rho_0) \\ J_{sp} &= J_{inc}(1 - \rho_0 \exp(-\rho_0^2)\sqrt{\pi}\,\mathrm{erfi}(\rho_0)) \\ J &= J_{inc}(1 - \tfrac{1}{2}\rho_0 \exp(-\rho_0^2)\sqrt{\pi}\,\mathrm{erfi}(\rho_0)), \end{aligned} \tag{27}$$

where erfi denotes Dawson's integral [12]

$$\mathrm{erfi}(x) \equiv \frac{2}{\sqrt{\pi}} \int_0^x \mathrm{d}t \exp(t^2). \tag{28}$$

These results, showing how the angular momenta depend on the strength of the crystal, as described by the ring radius ρ_0, are illustrated in figure 4. An interesting feature is that during the transformation to purely orbital angular momentum (section 4.1) the spin angular momentum reverses sign as it falls to zero, with a minimum value $J_{sp} = -0.285$ when $\rho_0 = 1.502$.

4.4. Large chirality or biaxiality

When $\rho_0 \gg 1$ or $\gamma \gg 1$, the oscillatory integral F (equation (23)) is small, and

$$\begin{aligned} J_{orb} &= \tfrac{1}{2} J_{inc}[1 - (\gamma/\rho_0)^2 \exp\{(\gamma/\rho_0)^2\} E_1\{(\gamma/\rho_0)^2\}] \\ J_{sp} &= J_{inc}[(\gamma/\rho_0)^2 \exp\{(\gamma/\rho_0)^2\} E_1\{(\gamma/\rho_0)^2\}] \\ J &= \tfrac{1}{2} J_{inc}[1 + (\gamma/\rho_0)^2 \exp\{(\gamma/\rho_0)^2\} E_1\{(\gamma/\rho_0)^2\}]. \end{aligned} \tag{29}$$

Figure 5 shows how this approximation describes the average of the oscillations of the angular momenta as a function of γ, which get weaker as ρ_0 increases.

4.5. Oscillatory corrections for large chirality or biaxiality

In the case just considered, the weak oscillations are given asymptotically by the behaviour of the integral F at its end-point $t = \gamma/\rho_0$. The zero-order term vanishes because of the factor $t - (\gamma/\rho_0)^2/t$, and the leading-order approximation, derived by two integrations by parts, is

$$\begin{aligned} J_{orb} &= \tfrac{1}{2} J_{inc}[1 - (\gamma/\rho_0)^2 \exp\{(\gamma/\rho_0)^2\} E_1\{(\gamma/\rho_0)^2\} \\ &\quad - \rho_0^2\,\mathrm{Re}[\exp(-2\mathrm{i}\gamma)/(\gamma + \mathrm{i}\rho_0^2)^2]] \\ J_{sp} &= J_{inc}[(\gamma/\rho_0)^2 \exp\{(\gamma/\rho_0)^2\} E_1\{(\gamma/\rho_0)^2\} \\ &\quad + \rho_0^2\,\mathrm{Re}[\exp(-2\mathrm{i}\gamma)/(\gamma + \mathrm{i}\rho_0^2)^2]] \\ J &= \tfrac{1}{2} J_{inc}[1 + (\gamma/\rho_0)^2 \exp\{(\gamma/\rho_0)^2\} E_1\{(\gamma/\rho_0)^2\} \\ &\quad + \rho_0^2\,\mathrm{Re}[\exp(-2\mathrm{i}\gamma)/(\gamma + \mathrm{i}\rho_0^2)^2]]. \end{aligned} \tag{30}$$

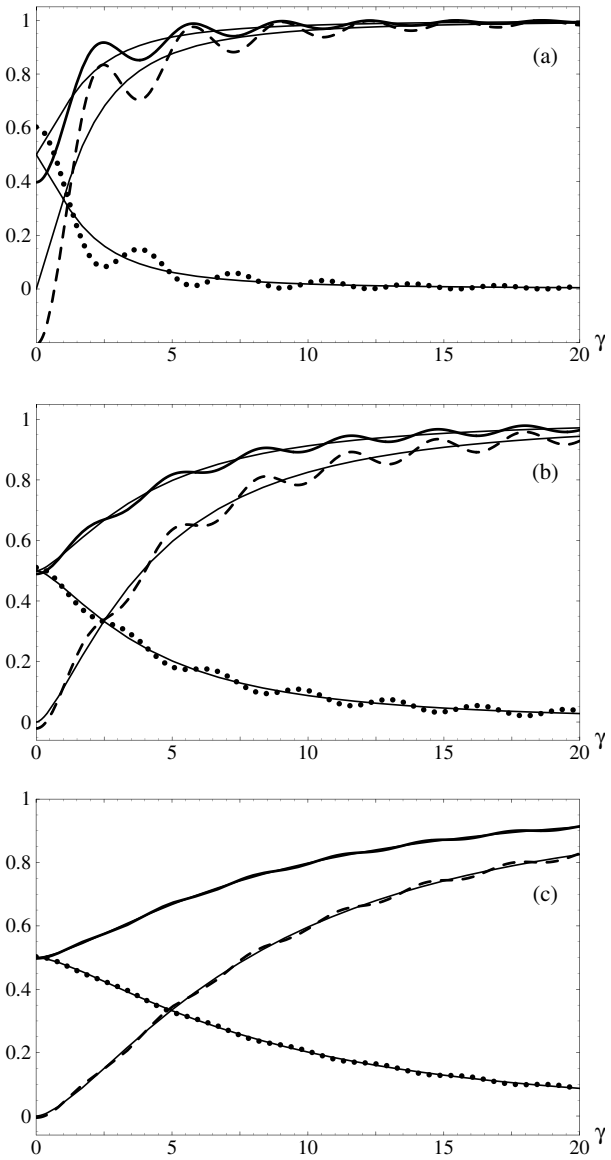

Figure 5. Angular momenta as a function of chirality γ, for (a) $\rho_0 = 2$, (b) $\rho_0 = 5$, (c) $\rho_0 = 10$. Exact computations from (21): thick dotted curves, J_{orb}; thick dashed curves, J_{sp}; thick continuous curves, J. Approximations (29): thin curves.

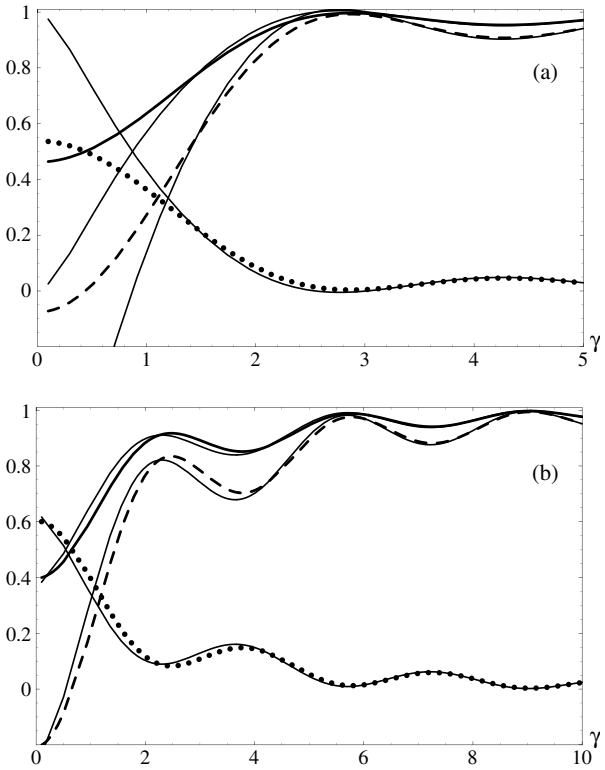

Figure 6. Angular momenta as a function of chirality γ, for (a) $\rho_0 = 1$ and (b) $\rho_0 = 2$. Exact computations from (21): thick dotted curves, J_{orb}; thick dashed curves, J_{sp}; thick continuous curves, J. Approximations (30): thin curves.

Figure 6 shows that this approximation captures the oscillations, with an accuracy that increases with ρ_0.

Physically, the oscillations with γ can be regarded as a consequence of interference between geometrical contributions from the two sheets of the wave surface, which, in contrast to those in the well developed ring case of section 4.1, are no longer in phase.

5. Concluding remarks

We have shown that for any biaxial crystal (i.e. $\rho_0 > 0$), with or without optical activity γ, the total angular momentum emerging from the slab is different from that incident on it. Therefore, the light must exert a torque on the slab, tending to rotate it about the incident beam direction. The magnitude of this torque is $J_{\text{inc}} - J$ multiplied by the rate of arrival of photons from the incident beam. It would be interesting to measure this.

A different torque arises from the fact that the cone and cylinder axes do not coincide with that of the incident beam (figure 1). This generates a torque about an axis in the plane of the slab and perpendicular to the incident beam, whose magnitude, is, for photon wavelength $\lambda = 2\pi/k$, the rate of arrival of photons multiplied by the angular momentum

$$J_1 = R_0 \times \text{photon momentum} = \frac{\hbar R_0}{\lambda}. \qquad (31)$$

This is much larger than the torque associated with the polarization changes we have been studying, since these are of order $\hbar$ or smaller, and $R_0 \gg \lambda$ for any situation involving conical refraction.

We have considered only the simplest case of a uniformly polarized incident beam with circular symmetry. The same techniques (based on (1) and (5)–(7)) can be applied straightforwardly to calculate the spin and orbital angular momenta for more complicated incident beams. An obvious example is the family of Laguerre–Gauss beams, where the intensity is circularly symmetric but the phase varies around the beam; in these cases, J_{inc} will have an orbital as well as a spin part. Another generalization would be to beams with non-circular intensity distributions, such as Gauss–Hermite beams. We leave these cases as exercises for interested readers.

Finally, we emphasize that our calculations have concerned the angular momenta outside the crystal. We have

not needed to address the tricky question of angular momentum within the crystal, which has been studied recently [17] for a beam inside a uniaxial crystal and travelling along its optic axis.

Acknowledgments

MVB and MM thank Professor Peter Török and the European Optical Society for their hospitality at Imperial College London, where this research started. MVB's research is supported by the Royal Society.

References

[1] Allen L, Barnett S M and Padgett M J 2003 *Optical Angular Momentum* (Bristol: Institute of Physics Publishing)
[2] Berry M V, Dennis M R and Soskin M S 2004 The plurality of optical singularities *J. Opt. A: Pure Appl. Opt.* **6** S155 (Editorial introduction to special issue)
[3] Hamilton W R 1837 Third supplement to an essay on the theory of systems of rays *Trans. R. Irish. Acad.* **17** 1–144
[4] Lloyd H 1833 On the phaenomena presented by light in its passage along the axes of biaxial crystals *Phil. Mag.* **2** 112–20
[5] Lloyd H 1833 Further experiments on the phaenomena presented by light in its passage along the axes of biaxial crystals *Phil. Mag.* **2** 207–10
[6] Born M and Wolf E 1959 *Principles of Optics* (London: Pergamon)
[7] Belskii A M and Khapalyuk A P 1978 Internal conical refraction of bounded light beams in biaxial crystals *Opt. Spectrosc. (USSR)* **44** 436–9
[8] Belsky A M and Stepanov M A 2002 Internal conical refraction of light beams in biaxial gyrotropic crystals *Opt. Commun.* **204** 1–6
[9] Berry M V 2004 Conical diffraction asymptotics: fine structure of Poggendorff rings and axial spike *J. Opt. A: Pure Appl. Opt.* **6** 289–300
[10] Berry M V 1998 Paraxial beams of spinning light *Singular Optics* (*SPIE* vol 3487) ed M S Soskin (Frunzenskoe, Crimea: SPIE Optical Engineering Press) pp 6–13
[11] Landau L D, Lifshitz E M and Pitaevskii L P 1984 *Electrodynamics of Continuous Media* (Oxford: Pergamon)
[12] Abramowitz M and Stegun I A 1972 *Handbook of Mathematical Functions* (Washington: National Bureau of Standards)
[13] Nye J F and Hajnal J V 1987 The wave structure of monochromatic electromagnetic radiation *Proc. R. Soc.* A **409** 21–36
[14] Nye J F 1999 *Natural Focusing and Fine Structure of Light: Caustics and Wave Dislocations* (Bristol: Institute of Physics Publishing)
[15] Berry M V and Dennis M R 2001 Polarization singularities in isotropic random waves *Proc. R. Soc.* A **457** 141–55
[16] Berry M V 2001 Geometry of phase and polarization singularities, illustrated by edge diffraction and the tides *Singular Optics 2000* (*SPIE* vol 4403) ed M Soskin (Alushta, Crimea: SPIE Optical Engineering Press) pp 1–12
[17] Ciattoni A, Cincotti L and Palma C 2003 Angular momentum dynamics of a paraxial beam in a uniaxial crystal *Phys. Rev.* E **67** 036618-1–10